

Article

Collocation Technique Based on Chebyshev Polynomials to Solve Emden–Fowler-Type Singular Boundary Value Problems with Derivative Dependence

Shabanam Kumari ¹, Arvind Kumar Singh ^{1,*} and Utsav Gupta ²

¹ Department of Mathematics, Institute of Science, Banaras Hindu University, Varanasi 221005, India; 92shabsharma@gmail.com

² Tanglin Trust School, 95 Portsdown Rd, Singapore 139299, Singapore; utsav.gupta@tts.edu.sg

* Correspondence: arvindks@bhu.ac.in

Abstract: In this work, an innovative technique is presented to solve Emden–Fowler-type singular boundary value problems (SBVPs) with derivative dependence. These types of problems have significant applications in applied mathematics and astrophysics. Initially, the differential equation is transformed into a Fredholm integral equation, which is then converted into a system of nonlinear equations using the collocation technique based on Chebyshev polynomials. Subsequently, an iterative numerical approach, such as Newton’s method, is employed on the system of nonlinear equations to obtain an approximate solution. Error analysis is included to assess the accuracy of the obtained solutions and provide insights into the reliability of the numerical results. Furthermore, we graphically compare the residual errors of the current method to the previously established method for various examples.

Keywords: Chebyshev polynomials; Emden–Fowler-type SBVPs; derivative dependence; functional approximation; Green’s function

MSC: 34B05; 34B15; 34B16; 65L10



Citation: Kumari, S.; Singh, A.K.; Gupta, U. Collocation Technique Based on Chebyshev Polynomials to Solve Emden–Fowler-Type Singular Boundary Value Problems with Derivative Dependence. *Mathematics* **2024**, *12*, 592. <https://doi.org/10.3390/math12040592>

Academic Editors: M. Filomena Teodoro and Marina Alexandra Pedro Andrade

Received: 3 January 2024

Revised: 11 February 2024

Accepted: 12 February 2024

Published: 17 February 2024



Copyright: © 2024 by the authors. Licensee MDPI, Basel, Switzerland. This article is an open access article distributed under the terms and conditions of the Creative Commons Attribution (CC BY) license (<https://creativecommons.org/licenses/by/4.0/>).

1. Introduction

Consider Emden–Fowler-type SBVPs with derivative dependence, as expressed by the following equation:

$$\begin{cases} (\rho(t)w'(t))' = \sigma(t) \phi(t, w(t), \rho(t)w'(t)), & t \in (0, 1), \\ w(0) = \beta_4 \text{ or } \lim_{t \rightarrow 0^+} \rho(t)w'(t) = 0, & \beta_1 w(1) + \beta_2 w'(1) = \beta_3, \end{cases} \quad (1)$$

where $\beta_1 > 0, \beta_2, \beta_3$, and β_4 are real constants. Here, $\phi(t, w(t), \rho(t)w'(t))$ is the source function dependent on both $w(t)$ and $w'(t)$.

The conditions $\rho(t) = t^b p(t)$, $p(0) \neq 0$, $\sigma(t) = t^a q(t)$, $q(0) \neq 0$, with $\rho(0) = 0$ and the allowance of $\sigma(t)$ to be discontinuous at $t = 0$, lead to a reduction of the problem to double SBVPs [1]. Such problems are prevalent in various areas of astrophysics, including thermal explosion modeling in a rectangular slab [2,3], heat source measurements in human heads [4], oxygen concentration within spherical cells [5], shallow membrane cap theory [6], heat conduction problems [7], unsteady Poiseuille flow in a pipe [8], electroelastic dynamic problems [9], and heat explosions [10].

Solving Emden–Fowler SBVPs with derivative dependence is crucial for predicting system behaviors, such as changes in pressure, density, or temperature within stars or gaseous spheres. The solutions provide valuable insights into the structure and evolution of these systems. Finding numerical solutions for derivative-dependent second-order singular differential equations is particularly challenging due to strong nonlinearity from

derivatives in the source function and the singular behavior at the origin. The motivation lies in developing numerical methods that require less computational effort while maintaining high accuracy. The collocation method has gained popularity with the widespread availability and efficiency of computers, being applied to problems in physics, engineering, and other fields.

The existence and uniqueness of the estimated solution of Equation (1) were readily obtained in [11–16] under the conditions of $\rho \in C[0, 1] \cap C^1(0, 1]$ with $\int_0^1 \frac{dt}{\rho(t)} < \infty$ and $\int_0^1 \sigma(t)dt < \infty$ for $\rho(t), \sigma(t) > 0$ on $(0, 1]$.

Several numerical methods have been developed to solve Equation (1) when $\phi(t, w, \rho w') = \phi(t, w)$, including the cubic spline method [17], the finite difference method [18–22], the Adomian decomposition method (ADM) [23–28], the B-spline collocation method [29,30], the classical polynomial approximation method [31], etc. However, there are limited techniques available for solving Emden–Fowler SBVPs with derivative dependence. In 2014, Singh et al. [26] discussed the Adomian decomposition technique to solve an original utilizing Green’s function. In 2018, Roul [32] presented an improved normal homotopy analysis method to solve derivative-dependent SBVPs, and in 2019, Roul et al. [33] discussed quintic spline interpolation. In 2020, Shahni et al. [34] established an approximate solution for Emden–Fowler-type SBVPs with derivative dependence using Bernstein polynomials. Upon examining existing techniques, limitations were identified, such as a significant amount of computational work, especially for nonlinear singular boundary value problems. Therefore, there is a need for more efficient numerical methods that can overcome these limitations and provide a more accurate solution for nonlinear singular boundary value problems.

This work introduces a constructive approach for solving Emden–Fowler-type SBVPs with derivative dependence. In Section 2, the differential equation is converted into its equivalent Fredholm integral form. In Section 3, a collocation technique based on Chebyshev polynomials (CCM) is employed to obtain the system of nonlinear equations upon transformation of the Fredholm integral equation. Subsequently, Newton’s method is implemented to solve the system and obtain the required solution. In Section 4, the algorithm for the methodology is provided for implementing the method. In Section 5, error analysis is included to assess the accuracy of the current method. In Section 6, the maximum absolute error of the current method is computed for various examples using L_∞ and L_2 norm. These numerical results are compared with those obtained using the existing BCM method [34]. The residual errors between CCM and a previously established method, i.e., BCM, are also compared graphically.

2. The Construction of the Method

The corresponding integral equations of the Emden–Fowler SBVPs are presented in this section.

2.1. Emden–Fowler SBVPs with Dirichlet–Robin Boundary Conditions

We consider the following differential equation:

$$\begin{cases} (\rho(t)w'(t))' = \sigma(t) \phi(t, w(t), \rho(t)w'(t)), & t \in (0, 1), \\ w(0) = \beta_4, \quad \beta_1 w(1) + \beta_2 w'(1) = \beta_3. \end{cases} \tag{2}$$

The equivalent Fredholm integral form of Equation (2) is

$$w(t) = \beta_4 + \frac{(\beta_3 - \beta_1\beta_4)}{\beta_1 h(1) + \beta_2 h'(1)} h(t) + \int_0^1 \kappa(t, \zeta) \sigma(\zeta) \phi(\zeta, w(\zeta), \rho(\zeta)w'(\zeta)) d\zeta, \quad t \in (0, 1), \tag{3}$$

where

$$\kappa(t, \zeta) = \begin{cases} h(t) - \left(\frac{\beta_1 h(\zeta) h(t)}{\beta_1 h(1) + \beta_2 h'(1)} \right), & t \leq \zeta, \\ h(\zeta) - \left(\frac{\beta_1 h(\zeta) h(t)}{\beta_1 h(1) + \beta_2 h'(1)} \right), & \zeta \leq t, \end{cases} \tag{4}$$

$$h(t) = \int_0^t \frac{1}{\rho(\zeta)} d\zeta, h(1) = \int_0^1 \frac{1}{\rho(\zeta)} d\zeta \text{ and } h'(1) = \frac{1}{\rho(1)}.$$

2.2. Emden–Fowler SBVPs with Neumann–Robin Boundary Conditions

We consider the following differential equation:

$$\begin{cases} (\rho(t)w'(t))' = \sigma(t) \phi\left(t, w(t), \rho(t)w'(t)\right), & t \in (0, 1) \\ \lim_{t \rightarrow 0^+} \rho(t)w'(t) = 0, & \beta_1 w(1) + \beta_2 w'(1) = \beta_3. \end{cases} \tag{5}$$

Its equivalent Fredholm integral form is

$$w(t) = \frac{\beta_3}{\beta_1} + \int_0^1 \kappa(t, \zeta) \sigma(\zeta) \phi\left(\zeta, w(\zeta), \rho(\zeta)w'(\zeta)\right) d\zeta, \quad t \in (0, 1), \tag{6}$$

where

$$\kappa(t, \zeta) = \begin{cases} \int_{\zeta}^1 \frac{1}{\rho(t)} dt + \frac{\beta_2}{\beta_1 \rho(1)}, & t \leq \zeta, \\ \int_{\zeta}^1 \frac{1}{\rho(t)} dt - \int_{\zeta}^t \frac{1}{\rho(t)} dt + \frac{\beta_2}{\beta_1 \rho(1)}, & \zeta \leq t. \end{cases} \tag{7}$$

3. Chebyshev Collocation Method (CCM)

This section includes the derivation of the CCM to approximate integral Equations (3) and (6).

Definition 1. Shifted Chebyshev polynomials (SCPs) are defined on $[0, 1]$ by introducing a new variable ($s = 2t - 1$) as

$$\begin{cases} \tau_0(t) = 1, \\ \tau_1(t) = 2t - 1, \\ \tau_n(t) = 2(2t - 1)\tau_{n-1}(t) - \tau_{n-2}(t). \end{cases} \tag{8}$$

We can approximate a function ($f(t) \in L^2[0, 1]$) by shifted Chebyshev polynomials (SCPs) as

$$f(t) = \sum_{r=0}^{\infty} c_r \tau_r(t). \tag{9}$$

For the purpose of numerical calculations, we take into account the initial $(n + 1)$ terms of the aforementioned expansion, and it becomes

$$f(t) \approx \sum_{r=0}^n c_r \tau_r(t) = \mathbf{A}^T \boldsymbol{\tau}(t), \tag{10}$$

where \mathbf{A} and $\boldsymbol{\tau}(t)$ are column vectors, as follows:

$$\mathbf{A} = [c_0, c_1, \dots, c_n]^T, \quad \boldsymbol{\tau}(t) = [\tau_0(t), \tau_1(t), \dots, \tau_n(t)]^T. \tag{11}$$

3.1. Dirichlet–Robin Boundary Conditions

To apply the current approach, we consider Equation (3) as

$$w(t) = \beta_4 + \frac{(\beta_3 - \beta_1\beta_4)}{\beta_1h(1) + \beta_2h'(1)}h(t) + \int_0^1 \kappa(t, \zeta) \sigma(\zeta) \phi(\zeta, w(\zeta), \rho(\zeta)w'(\zeta))d\zeta, \quad t \in (0, 1).$$

We take

$$z(t) = \phi\left(t, w(t), \rho(t)w'(t)\right). \tag{12}$$

We approximate $w(t)$, $w'(t)$ and $z(t)$ by using Equation (10),

$$w(t) \approx \sum_{r=0}^n c_r \tau_r(t), \tag{13}$$

$$w'(t) \approx \sum_{r=0}^n c_r \tau'_r(t), \tag{14}$$

$$z(t) \approx \sum_{r=0}^n d_r \tau_r(t). \tag{15}$$

By substituting Equations (12), (13), and (15) into (3), we obtain

$$\sum_{r=0}^n c_r \tau_r(t) = \beta_4 + \frac{(\beta_3 - \beta_1\beta_4)}{\beta_1h(1) + \beta_2h'(1)}h(t) + \sum_{r=0}^n d_r \int_0^1 \kappa(t, \zeta) \sigma(\zeta) \tau_r(\zeta) d\zeta. \tag{16}$$

It can be expressed as

$$\sum_{r=0}^n c_r \tau_r(t) = \beta_4 + \frac{(\beta_3 - \beta_1\beta_4)}{\beta_1h(1) + \beta_2h'(1)}h(t) + \sum_{r=0}^n d_r K_r(t), \tag{17}$$

where

$$K_r(t) = \int_0^1 \kappa(t, \zeta) \sigma(\zeta) \tau_r(\zeta) d\zeta, \quad r = 0, 1, \dots, n. \tag{18}$$

We differentiate Equation (17) with respect to t as

$$\sum_{r=0}^n c_r \tau'_r(t) = \frac{(\beta_3 - \beta_1\beta_4)}{\beta_1h(1) + \beta_2h'(1)}h'(t) + \sum_{r=0}^n d_r K'_r(t), \tag{19}$$

where

$$K'_r(t) = \frac{d}{dt} \left(\int_0^1 \kappa(t, \zeta) \sigma(\zeta) \tau_r(\zeta) d\zeta \right), \quad r = 0, 1, \dots, n. \tag{20}$$

Then, by plugging Equations (13)–(15) into (12), we obtain

$$\sum_{r=0}^n d_r \tau_r(t) = \phi\left(t, \sum_{r=0}^n c_r \tau_r(t), \rho(t) \sum_{r=0}^n c_r \tau'_r(t)\right). \tag{21}$$

By substituting Equations (17) and (19) into (21) and inserting the collocation points $(t_s = \frac{1}{2} \left\{ \cos \left(\frac{(2s+1)\pi}{2n} \right) + 1 \right\}, s = 0, 1, \dots, n)$ into Equation (21), we have

$$\sum_{r=0}^n d_r \tau_r(t_s) - \phi \left(t_s, \beta_4 + \frac{(\beta_3 - \beta_1 \beta_4)}{\beta_1 h(1) + \beta_2 h'(1)} h(t_s) + \sum_{r=0}^n d_r K_r(t_s), \right. \\ \left. \rho(t_s) \frac{(\beta_3 - \beta_1 \beta_4)}{\beta_1 h(1) + \beta_2 h'(1)} h'(t_s) + \sum_{r=0}^n d_r K'_r(t_s) \right) = 0, \quad s = 0, 1, \dots, n, \quad (22)$$

where d_0, d_1, \dots, d_n are unknowns.

In order to obtain the approximate solution of Equation (3), we substitute the unknown coefficients in Equations (17) and (19), which are obtained by applying the iteration approach to Equation (22).

Note that a desired accuracy (ϵ) of Newton’s method can be obtained by using the stopping criteria ($\|\tau^{[s+1]} - \tau^{[s]}\| < \epsilon$).

3.2. Neumann–Robin Boundary Conditions

Consider Equation (6) as

$$w(t) = \frac{\beta_3}{\beta_1} + \int_0^1 \kappa(t, \zeta) \sigma(\zeta) \phi(\zeta, w(\zeta), \rho(\zeta)w'(\zeta)) d\zeta, \quad t \in (0, 1). \quad (23)$$

Using similar steps as in the previous subsection, we input the expressions from Equations (13) and (14) into (23), yielding

$$\sum_{r=0}^n c_r \tau_r(t) = \frac{\beta_3}{\beta_1} + \sum_{r=0}^n d_r \int_0^1 \kappa(t, \zeta) \sigma(\zeta) \tau_r(\zeta) d\zeta, \quad (24)$$

which can be represented as

$$\sum_{r=0}^n c_r \tau_r(t) = \frac{\beta_3}{\beta_1} + \sum_{r=0}^n d_r K_r(t) \quad (25)$$

and

$$\sum_{r=0}^n c_r \tau'_r(t) = \sum_{r=0}^n d_r K'_r(t). \quad (26)$$

Then, by plugging Equations (25) and (26) into (21) and inserting the collocation points $(t_s = \frac{1}{2} \left\{ \cos \left(\frac{(2s+1)\pi}{2n} \right) + 1 \right\}, s = 0, 1, \dots, n)$, we obtain

$$\sum_{r=0}^n d_r \tau_r(t_s) - \phi \left(t_s, \frac{\beta_3}{\beta_1} + \sum_{r=0}^n d_r K_r(t_s), \rho(t_s) \sum_{r=0}^n d_r K'_r(t_s) \right) = 0, \quad s = 0, 1, \dots, n. \quad (27)$$

In order to obtain the approximate solutions of Equation (23), we substitute the unknown coefficients (d_0, d_1, \dots, d_n) into Equations (25) and (26), which are obtained by applying Newton’s method [35] to Equation (27).

4. Algorithm of the Methodology

The procedure for determining unknown coefficients in the CCM method is outlined by the following algorithm:

1. Input the degree of the Chebyshev polynomials, i.e., n .
2. Approximate $w(t)$ and $\phi(t, w(t), \rho(t)w'(t))$ via Equation (13).

3. Input the collocation points $(t_s = \frac{1}{2} \left\{ \cos\left(\frac{(2s+1)\pi}{2n}\right) + 1 \right\}, s = 0, 1, \dots, n)$.
4. Obtain a nonlinear equation in unknowns, i.e., d_0, d_1, \dots, d_n .
5. Via Newton’s method, the numerical solution is obtained.

5. Error Analysis

Let the norm of the Banach space $(X = C[0, 1] \cap C^1(0, 1])$ be defined as

$$\|w\| = \max\{\|w\|_0, \|w\|_1\}, \quad w \in X, \tag{28}$$

where

$$\|w\|_0 = \max_{t \in [0,1]} |w(t)|, \tag{29}$$

$$\|w\|_1 = \max_{t \in [0,1]} |\rho(t) w'(t)|. \tag{30}$$

Theorem 1. *Let the sequence $\{\tau_n(f)\}$ converge uniformly to $f(t) \in C[0, 1]$, where $\tau_n(f) = \sum_{r=0}^n c_r \tau_r(t)$ is the Chebyshev approximation function. Then, for a given $\epsilon > 0$, there exists a number (n) such that*

$$\|\tau_n(f) - f\| < \epsilon.$$

Proof of Theorem 1. The proof is provided in [36]. □

Theorem 2. *Consider a bounded function (f) in $[0, 1]$ and that its second derivative exists. Then, the error bound can be derived as*

$$\|\tau_n(f) - f\| \leq \frac{\|f''\|}{2n} \max_{t \in [0,1]} (t(1-t)) = \frac{\|f''\|}{8n}, \tag{31}$$

which exhibits the rate of convergence $(1/n)$ for Chebyshev’s approximation function [37], provided $f''(t) \neq 0$.

Proof of Theorem 2. The proof is provided in [38]. □

Theorem 3. *Consider a Banach space (X) with the norm as defined in Equation (28). Let $w_n(t)$ and $w(t)$ represent the approximate and exact solutions of the integral Equation (3), respectively. Furthermore, the nonlinear function $\phi(t, w(t), \rho w'(t))$ also satisfies the Lipschitz condition, as follows:*

$$|\phi(t, w, \rho w') - \phi(t, w_n, \rho w'_n)| \leq l_1 |w - w_n| + l_2 |\rho(w' - w'_n)|, \tag{32}$$

where l_1 and l_2 are the Lipschitz constants. Then, for the CCM, the estimated error bound is determined as

$$\|w - w_n\| \leq \frac{v l m}{4n}, \tag{33}$$

where $l = \max(l_1, l_2)$, $m = \max(m_1, m_2)$, $v = \|w''\|$,

$$m_1 = \max_{t \in [0,1]} \left| \int_0^1 \kappa(t, \zeta) \sigma(\zeta) d\zeta \right| \leq \infty, \tag{34}$$

$$m_2 = \max_{t \in [0,1]} \left| \int_0^1 \rho(t) \kappa_t(t, \zeta) \sigma(\zeta) d\zeta \right| \leq \infty. \tag{35}$$

Proof of Theorem 3. Consider

$$\begin{aligned} \|w - w_n\|_0 &= \max_{t \in [0,1]} \left| \int_0^1 \kappa(t, \zeta) \sigma(\zeta) \left(\phi(\zeta, w(\zeta), w'(\zeta)) - \phi(\zeta, w_n(\zeta), \rho(\zeta) w'_n(\zeta)) \right) d\zeta \right| \\ &= \max_{\zeta \in [0,1]} \left| \phi(\zeta, w(\zeta), \rho(\zeta) w'(\zeta)) - \phi(\zeta, w_n(\zeta), \rho(\zeta) w'_n(\zeta)) \right| \\ &\quad \times \max_{t \in [0,1]} \left| \int_0^1 \kappa(t, \zeta) \sigma(\zeta) d\zeta \right|. \end{aligned}$$

Using Equations (32) and (34), we obtain

$$\begin{aligned} \|w - w_n\|_0 &\leq m_1 \max_{\zeta \in [0,1]} l_1 |(w(\zeta) - w_n(\zeta))| + l_2 |\rho(\zeta)(w'(\zeta) - w'_n(\zeta))| \\ &\leq 2lm_1 \max \left(\|w - w_n\|_0, \|w - w_n\|_1 \right) \\ &= 2lm_1 \|w - w_n\|. \end{aligned} \tag{36}$$

Similarly, we consider

$$\begin{aligned} \|w - w_n\|_1 &= \max_{t \in [0,1]} \left| \int_0^1 \rho(\zeta) \kappa_t(t, \zeta) \sigma(\zeta) \left(\phi(\zeta, w(\zeta), w'(\zeta)) - \phi(\zeta, w_n(\zeta), \rho(\zeta) w'_n(\zeta)) \right) d\zeta \right| \\ &= \max_{\zeta \in [0,1]} \left| \phi(\zeta, w(\zeta), \rho(\zeta) w'(\zeta)) - \phi(\zeta, w_n(\zeta), \rho(\zeta) w'_n(\zeta)) \right| \\ &\quad \times \max_{t \in [0,1]} \left| \int_0^1 \rho(t) \kappa_t(t, \zeta) \sigma(\zeta) d\zeta \right|. \end{aligned}$$

Using Equations (32) and (35), we have

$$\begin{aligned} \|w - w_n\|_1 &\leq m_2 \max_{\zeta \in [0,1]} l_1 |(w(\zeta) - w_n(\zeta))| + l_2 |\rho(\zeta)(w'(\zeta) - w'_n(\zeta))| \\ &\leq 2lm_2 \max \left(\|w - w_n\|_0, \|w - w_n\|_1 \right) \\ &= 2lm_2 \|w - w_n\|. \end{aligned} \tag{37}$$

From Equations (36) and (37), we have

$$\begin{aligned} \|w - w_n\| &= \max \left(\|w - w_n\|_0, \|w - w_n\|_1 \right) \\ &\leq \max \left(2lm_1 \|w - w_n\|_0, 2lm_2 \|w - w_n\|_1 \right) \\ &\leq 2lm \|w - w_n\| \\ &= 2lm \max_{\zeta \in [0,1]} \|w - w_n\|. \end{aligned} \tag{38}$$

Utilizing the CCM, we obtain the approximate solution ($\tau_n(w(t))$) of Equations (3) and (6). We replace $w_n(\zeta)$ with the Chebyshev solution ($\tau_n(w(\zeta))$), Equation (38) reduces to

$$\begin{aligned} \|w - w_n\| &\leq 2lm \max_{\zeta \in [0,1]} \|w(\zeta) - \tau_n(w(\zeta))\| \\ &\leq 2lm \|w - \tau_n(w)\|. \end{aligned} \tag{39}$$

Replacing f with w and t with ζ in Equation yields (31)

$$\|\tau_n(w) - w\| \leq \frac{\|w''\|}{2n} \max_{\zeta \in [0,1]} (\zeta(1 - \zeta)) = \frac{\|w''\|}{8n}. \tag{40}$$

If $v = \|w''\|$, then Equation (40) becomes

$$\|\tau_n(w) - w\| \leq \frac{v}{8n}. \tag{41}$$

Inputting Equation (41) into Equation (39), we obtain

$$\begin{aligned} \|w - w_n\| &\leq 2lm\left(\frac{v}{8n}\right) \\ &= \frac{vlm}{4n}. \end{aligned} \tag{42}$$

□

6. Numerical Illustration

We utilized MATLAB (R2015a) to determine maximum absolute errors using both L_∞ and L_2 norms for various examples to assess the accuracy of the current approach. Subsequently, we compared these results with those obtained using the BCM in the different tables and also graphically compared residual errors. We define L_∞ and L_2 norm errors as follows:

$$L_\infty = \max_{t \in [0,1]} |w(t) - w_n(t)|,$$

and

$$L_2 = \left(\sum_{j=1}^m |w(t_j) - w_n(t_j)|^2 \right)^{1/2},$$

where $w_n(t)$ and $w(t)$ represent the approximate and exact solutions, respectively.

Furthermore, the residual error is defined as:

$$\begin{aligned} r_n(t) &= |(\rho(t)w'_n(t))' - \sigma(t) \phi(t, w_n(t), \rho(t)w'_n(t))|, \\ R_n(t) &= |(\rho(t)w'_n(t))' - \sigma(t) \phi(t, w_n(t), \rho(t)w'_n(t))|, \end{aligned}$$

where $r_n(t)$ and $R_n(t)$ are obtained by using the CCM and the BCM, respectively.

Example 1.

$$\begin{cases} (t^b w')' = t^{b+q-2} (qtw' + q(b+q-1)w), & t \in (0, 1), \\ w(0) = 1, & w(1) = e. \end{cases} \tag{43}$$

The equivalent integral form is

$$w(t) = 1 + \frac{e-1}{(1-b)^2} t^{1-b} + \int_0^1 \kappa(t, \zeta) \zeta^{b+q-2} \left(q\zeta w' + q(b+q-1)w(\zeta) \right) d\zeta,$$

where

$$\kappa(t, \zeta) = \begin{cases} \frac{t^{1-b}}{1-b}(1 - \zeta^{1-b}), & t \leq \zeta, \\ \frac{\zeta^{1-b}}{1-b}(1 - t^{1-b}), & \zeta \leq t. \end{cases}$$

The exact solution of differential Equation (43) is $w(t) = e^{t^q}$.

We present a comparison of errors using the L_∞ norm of the CCM with the BCM for $q = 1$ and $q = 2.5$ in Tables 1 and 2, respectively, and a comparison of errors using the L_2 norm of the CCM with the BCM for $q = 1$ and $q = 2.5$ in Tables 3 and 4, respectively, for Example 1. We note that achieving the desired level of accuracy is more effectively accomplished with the CCM compared to the BCM. Furthermore, Figure 1 illustrates a comparison of residual errors between the current technique and the BCM, revealing that the residual errors of the CCM are significantly lower than those of the BCM.

Table 1. Comparison of errors using the L_∞ norm for $q = 1$ in Equation (43).

n	$b = 0.25$		$b = 0.5$		$b = 0.75$	
	CCM	BCM	CCM	BCM	CCM	BCM
4	9.41×10^{-6}	3.38×10^{-5}	1.10×10^{-5}	3.99×10^{-5}	1.27×10^{-5}	5.04×10^{-5}
5	2.93×10^{-7}	1.66×10^{-6}	3.26×10^{-7}	2.08×10^{-6}	3.59×10^{-7}	2.58×10^{-6}
6	6.35×10^{-9}	1.66×10^{-6}	6.69×10^{-9}	9.25×10^{-8}	7.00×10^{-9}	1.13×10^{-7}
7	1.88×10^{-10}	3.02×10^{-9}	2.01×10^{-10}	3.68×10^{-9}	2.13×10^{-10}	4.48×10^{-9}
8	3.90×10^{-12}	1.07×10^{-10}	4.04×10^{-12}	1.30×10^{-10}	4.13×10^{-12}	1.57×10^{-10}
9	1.17×10^{-13}	3.50×10^{-12}	1.27×10^{-13}	4.24×10^{-12}	1.36×10^{-13}	5.11×10^{-12}
10	2.25×10^{-15}	1.04×10^{-13}	2.40×10^{-15}	1.25×10^{-13}	2.53×10^{-15}	1.51×10^{-13}
11	2.99×10^{-16}	–	3.26×10^{-16}	–	3.41×10^{-16}	–

Table 2. Comparison of errors using the L_∞ norm for $q = 2.5$ in Equation (43).

n	$b = 0.25$		$b = 0.5$		$b = 0.75$	
	CCM	BCM	CCM	BCM	CCM	BCM
4	1.44×10^{-3}	2.10×10^{-3}	1.49×10^{-3}	2.17×10^{-3}	1.54×10^{-3}	2.23×10^{-3}
5	1.73×10^{-4}	3.88×10^{-4}	1.78×10^{-4}	3.99×10^{-4}	1.83×10^{-4}	4.10×10^{-4}
6	2.90×10^{-5}	6.91×10^{-5}	2.97×10^{-5}	7.13×10^{-5}	3.04×10^{-5}	7.34×10^{-5}
7	4.02×10^{-6}	1.25×10^{-5}	4.09×10^{-6}	1.28×10^{-5}	4.15×10^{-6}	1.32×10^{-5}
8	6.82×10^{-7}	2.20×10^{-6}	6.95×10^{-7}	2.27×10^{-6}	7.08×10^{-7}	2.34×10^{-6}
9	6.17×10^{-8}	3.61×10^{-7}	6.22×10^{-8}	3.70×10^{-7}	6.26×10^{-8}	3.79×10^{-7}
10	2.00×10^{-8}	7.16×10^{-8}	2.08×10^{-8}	7.94×10^{-8}	2.16×10^{-8}	9.53×10^{-8}
11	2.21×10^{-9}	–	2.39×10^{-9}	–	2.58×10^{-9}	–

Table 3. Comparison of errors using the L_2 norm for $q = 1$ in Equation (43).

n	$b = 0.25$		$b = 0.5$		$b = 0.75$	
	CCM	BCM	CCM	BCM	CCM	BCM
3	3.35×10^{-4}	1.23×10^{-3}	3.87×10^{-4}	1.42×10^{-3}	4.42×10^{-4}	1.63×10^{-3}
4	1.20×10^{-5}	6.46×10^{-5}	1.35×10^{-5}	7.40×10^{-5}	1.50×10^{-5}	8.42×10^{-5}
5	3.72×10^{-7}	3.22×10^{-6}	4.05×10^{-7}	3.66×10^{-6}	4.37×10^{-7}	4.14×10^{-6}
6	1.01×10^{-8}	3.22×10^{-6}	1.07×10^{-8}	1.55×10^{-7}	1.13×10^{-8}	1.74×10^{-7}
7	2.39×10^{-10}	5.52×10^{-9}	2.53×10^{-10}	6.21×10^{-9}	2.65×10^{-10}	6.94×10^{-9}
8	5.96×10^{-12}	1.93×10^{-10}	6.34×10^{-12}	2.16×10^{-10}	6.70×10^{-12}	2.41×10^{-10}
9	1.48×10^{-13}	6.43×10^{-12}	1.53×10^{-13}	7.17×10^{-12}	1.62×10^{-13}	7.97×10^{-12}
10	3.24×10^{-15}	1.90×10^{-13}	3.38×10^{-15}	2.11×10^{-13}	3.53×10^{-15}	2.34×10^{-13}
11	5.38×10^{-16}	–	5.52×10^{-16}	–	5.89×10^{-16}	–

Table 4. Comparison of errors using the L_2 norm for $q = 2.5$ in Equation (43).

n	$b = 0.25$		$b = 0.5$		$b = 0.75$	
	CCM	BCM	CCM	BCM	CCM	BCM
3	1.53×10^{-2}	2.02×10^{-2}	1.67×10^{-2}	2.18×10^{-2}	1.85×10^{-2}	2.37×10^{-2}
4	2.25×10^{-3}	2.70×10^{-3}	2.35×10^{-3}	2.84×10^{-3}	2.45×10^{-3}	2.99×10^{-3}
5	3.01×10^{-4}	5.27×10^{-4}	3.10×10^{-4}	5.72×10^{-4}	3.19×10^{-4}	6.29×10^{-4}
6	4.62×10^{-5}	8.16×10^{-5}	4.75×10^{-5}	8.60×10^{-5}	4.87×10^{-5}	9.06×10^{-5}
7	6.23×10^{-6}	1.78×10^{-5}	6.36×10^{-6}	1.93×10^{-5}	6.49×10^{-6}	2.13×10^{-5}
8	1.08×10^{-6}	2.78×10^{-6}	1.10×10^{-6}	2.93×10^{-6}	1.13×10^{-6}	3.10×10^{-6}
9	1.07×10^{-7}	5.18×10^{-7}	1.07×10^{-7}	5.52×10^{-7}	1.08×10^{-7}	5.93×10^{-7}
10	3.87×10^{-8}	1.20×10^{-7}	4.01×10^{-8}	1.33×10^{-7}	4.16×10^{-8}	1.48×10^{-7}
11	5.64×10^{-9}	–	6.09×10^{-9}	–	6.56×10^{-9}	–

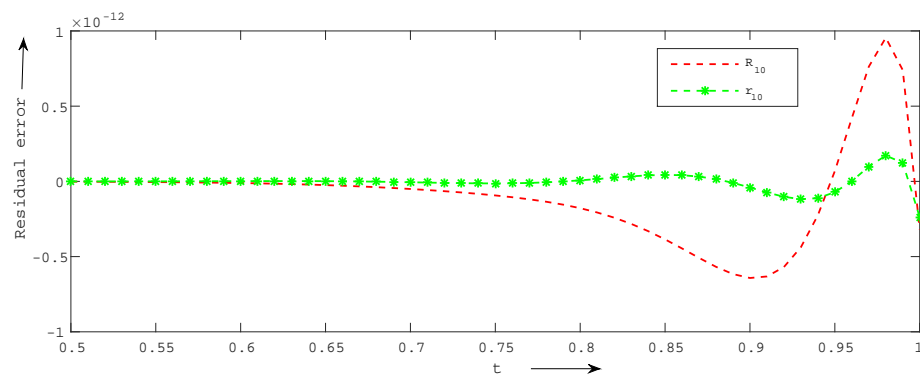


Figure 1. Comparison of residual errors obtained by the CCM and the previously established BCM for Example 1.

Example 2.

$$\begin{cases} (t^b w')' = t^{b-1} (-t w' e^w - b e^w), & t \in (0, 1], \\ w(0) = \ln\left(\frac{1}{2}\right), & w(1) = \ln\left(\frac{1}{3}\right). \end{cases} \tag{44}$$

Its equivalent integral form is

$$w(t) = \ln\left(\frac{1}{2}\right) + \frac{\left(\ln\left(\frac{1}{3}\right) - \ln\left(\frac{1}{2}\right)\right)}{(1-b)^2} t^{1-b} + \int_0^1 \kappa(t, \zeta) \zeta^{b-1} \left(-\zeta w'(\zeta) e^{w(\zeta)} - b e^{w(\zeta)}\right) d\zeta,$$

where

$$\kappa(t, \zeta) = \begin{cases} \frac{t^{1-b}}{1-b} (1 - \zeta^{1-b}), & t \leq \zeta, \\ \frac{\zeta^{1-b}}{1-b} (1 - t^{1-b}), & \zeta \leq t. \end{cases}$$

The exact solution of differential Equation (44) is

$$w(t) = \ln\left(\frac{1}{t+2}\right).$$

We present a comparison of errors of the CCM with those of the BCM for $q = 1$ using the L_∞ and L_2 norms in Tables 5 and 6, respectively for Example 2. We note that achieving the desired level of accuracy is more effectively accomplished with the CCM compared to the BCM. Furthermore, Figure 2 illustrates a comparison of residual errors between the current technique and the BCM, revealing that the residual errors of the CCM are significantly lower than those of the BCM.

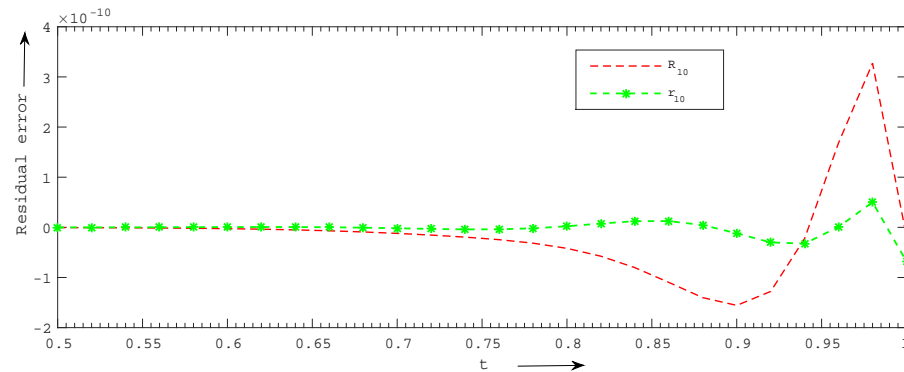


Figure 2. Comparison of residual errors obtained by the CCM and the BCM for Example 2.

Table 5. Comparison of errors using the L_∞ norm for $q = 1$ in Equation (44).

n	$b = 0.25$		$b = 0.5$		$b = 0.75$	
	CCM	BCM	CCM	BCM	CCM	BCM
4	2.45×10^{-6}	7.82×10^{-6}	3.03×10^{-6}	1.06×10^{-5}	3.82×10^{-6}	1.52×10^{-5}
5	1.89×10^{-7}	1.03×10^{-6}	2.21×10^{-7}	1.38×10^{-6}	2.67×10^{-7}	1.94×10^{-6}
6	1.10×10^{-8}	1.34×10^{-7}	1.28×10^{-8}	1.77×10^{-7}	1.58×10^{-8}	2.43×10^{-7}
7	1.06×10^{-9}	1.76×10^{-8}	1.20×10^{-9}	2.31×10^{-7}	1.37×10^{-9}	3.17×10^{-8}
8	7.94×10^{-11}	2.30×10^{-9}	8.79×10^{-11}	3.00×10^{-9}	1.09×10^{-10}	4.07×10^{-9}
9	1.04×10^{-11}	3.06×10^{-10}	1.19×10^{-11}	3.99×10^{-10}	1.37×10^{-11}	5.42×10^{-10}
10	8.66×10^{-13}	4.05×10^{-11}	9.66×10^{-13}	5.27×10^{-11}	1.10×10^{-12}	7.14×10^{-11}
11	5.61×10^{-14}	–	6.07×10^{-14}	–	6.68×10^{-14}	–

Table 6. Comparison of errors using the L_2 norm for $q = 1$ in Equation (44).

n	$b = 0.25$		$b = 0.5$		$b = 0.75$	
	CCM	BCM	CCM	BCM	CCM	BCM
3	3.90×10^{-5}	1.25×10^{-4}	4.86×10^{-5}	1.62×10^{-4}	6.22×10^{-5}	2.17×10^{-4}
4	2.97×10^{-6}	1.42×10^{-5}	3.58×10^{-6}	1.82×10^{-5}	4.43×10^{-6}	2.40×10^{-5}
5	2.26×10^{-7}	1.79×10^{-6}	2.61×10^{-7}	2.27×10^{-6}	3.12×10^{-7}	2.98×10^{-6}
6	1.73×10^{-8}	2.21×10^{-7}	1.97×10^{-8}	2.78×10^{-7}	2.34×10^{-8}	3.62×10^{-7}
7	1.30×10^{-9}	2.92×10^{-8}	1.49×10^{-9}	3.66×10^{-8}	1.78×10^{-9}	4.75×10^{-8}
8	1.21×10^{-10}	3.76×10^{-9}	1.38×10^{-10}	4.67×10^{-9}	1.64×10^{-10}	6.04×10^{-9}
9	1.25×10^{-11}	5.09×10^{-10}	1.39×10^{-11}	6.33×10^{-10}	1.59×10^{-11}	8.17×10^{-10}
10	1.12×10^{-12}	6.71×10^{-11}	1.23×10^{-12}	8.31×10^{-11}	1.42×10^{-12}	1.07×10^{-10}
11	7.93×10^{-14}	–	9.37×10^{-14}	–	1.17×10^{-13}	–

Example 3.

$$\begin{cases} (t^b w')' = -t^{b+q-2} \left(q t w' e^w + q(b+q-1)e^w \right), & t \in (0, 1], \\ w(0) = \ln\left(\frac{1}{4}\right), & w(1) = \ln\left(\frac{1}{5}\right). \end{cases} \quad (45)$$

Its integral form is

$$w(t) = \ln\left(\frac{1}{4}\right) + \frac{\left(\ln\left(\frac{1}{5}\right) - \ln\left(\frac{1}{4}\right)\right)}{(1-b)^2} t^{1-b} + \int_0^1 \kappa(t, \zeta) \zeta^{b+q-2} \left(q\zeta w'(\zeta)e^{w(\zeta)} + q(b+q-1)e^{w(\zeta)} \right) d\zeta,$$

where

$$\kappa(t, \zeta) = \begin{cases} \frac{t^{1-b}}{1-b} (1 - \zeta^{1-b}), & t \leq \zeta, \\ \frac{\zeta^{1-b}}{1-b} (1 - t^{1-b}), & \zeta \leq t. \end{cases}$$

The exact solution of differential Equation (45) is

$$w(t) = \ln\left(\frac{1}{4 + t^q}\right).$$

We present a comparison of errors using the L_∞ and L_2 norms of the CCM with those of the BCM for $q = 1$ for Example 3 in Tables 7 and 8, respectively. We clearly observe that achieving the desired level of accuracy is more effectively accomplished with the CCM compared to the BCM. Furthermore, Figure 3 illustrates a comparison of residual errors between the current technique and the BCM, revealing that the residual errors of the CCM are significantly lower than those of the BCM.

Table 7. Comparison of errors using the L_∞ norm for $q = 1$ in Equation (45).

n	$b = 0.25$		$b = 0.5$		$b = 0.75$	
	CCM	BCM	CCM	BCM	CCM	BCM
4	7.08×10^{-8}	2.37×10^{-7}	8.62×10^{-8}	3.13×10^{-7}	1.06×10^{-7}	4.38×10^{-7}
5	2.98×10^{-9}	1.69×10^{-8}	3.45×10^{-9}	2.25×10^{-8}	4.08×10^{-9}	3.09×10^{-8}
6	9.62×10^{-11}	1.21×10^{-9}	1.09×10^{-10}	1.58×10^{-9}	1.31×10^{-10}	2.13×10^{-9}
7	5.33×10^{-12}	8.82×10^{-11}	5.94×10^{-12}	1.14×10^{-10}	6.69×10^{-12}	1.53×10^{-10}
8	2.18×10^{-13}	6.35×10^{-12}	2.27×10^{-13}	8.17×10^{-12}	2.88×10^{-13}	1.09×10^{-11}
9	1.50×10^{-14}	4.66×10^{-13}	1.97×10^{-14}	6.00×10^{-13}	4.47×10^{-14}	8.00×10^{-13}
10	1.78×10^{-15}	3.41×10^{-14}	1.41×10^{-14}	4.38×10^{-14}	2.48×10^{-15}	5.81×10^{-14}

Table 8. Comparison of errors using the L_2 norm for $q = 1$ in Equation (45).

n	$b = 0.25$		$b = 0.5$		$b = 0.75$	
	CCM	BCM	CCM	BCM	CCM	BCM
3	2.07×10^{-6}	7.01×10^{-6}	2.53×10^{-6}	5.75×10^{-4}	3.15×10^{-6}	1.16×10^{-5}
4	8.67×10^{-8}	4.34×10^{-7}	1.02×10^{-7}	5.44×10^{-7}	1.24×10^{-7}	7.00×10^{-7}
5	3.65×10^{-9}	3.01×10^{-8}	4.16×10^{-9}	3.74×10^{-8}	4.84×10^{-9}	4.80×10^{-8}
6	1.56×10^{-10}	2.04×10^{-9}	1.75×10^{-10}	2.52×10^{-9}	2.02×10^{-10}	3.19×10^{-9}
7	6.55×10^{-12}	1.49×10^{-10}	7.35×10^{-12}	1.83×10^{-10}	8.52×10^{-12}	2.32×10^{-10}
8	3.35×10^{-13}	1.05×10^{-11}	3.77×10^{-13}	1.29×10^{-11}	4.35×10^{-13}	1.62×10^{-11}
9	1.91×10^{-14}	7.90×10^{-13}	2.09×10^{-14}	9.65×10^{-13}	2.34×10^{-14}	1.21×10^{-12}
10	1.07×10^{-15}	5.75×10^{-14}	1.17×10^{-15}	7.00×10^{-14}	1.33×10^{-15}	8.78×10^{-14}

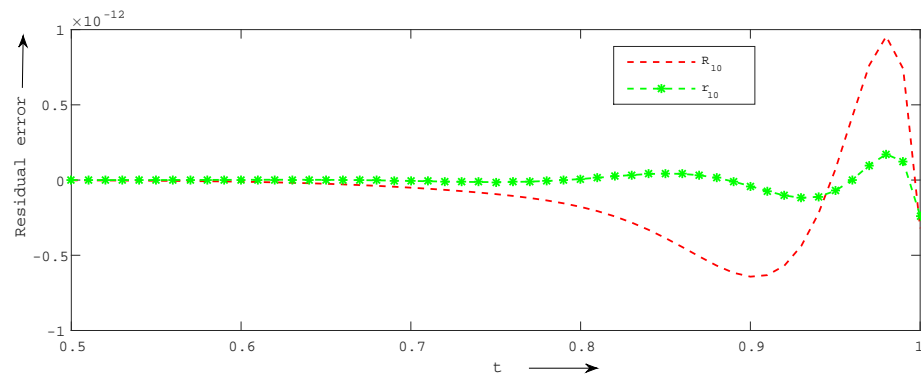


Figure 3. Comparison of residual errors obtained by the CCM and the BCM for Example 3.

Example 4.

$$\begin{cases} (t^b w')' = t^{b+q-2} (tw' + (b+q-1)w), & t \in (0, 1], \quad q > 0, \\ \lim_{t \rightarrow 0^+} r(t)w'(t) = 0, & w(1) = e. \end{cases} \tag{46}$$

The equivalent integral form is

$$w(t) = e + \int_0^1 \kappa(t, \zeta) \zeta^{b+q-2} \left(\zeta w'(\zeta) + (b+q-1)w(\zeta) \right) d\zeta,$$

where

$$\kappa(t, \zeta) = \begin{cases} \frac{1}{1-b} (1 - \zeta^{1-b}), & t \leq \zeta, \\ \frac{1}{1-b} (1 - t^{1-b}), & \zeta \leq t. \end{cases}$$

The exact solution of differential Equation (46) is $w(t) = e^{t^q}$.

We present a comparison of errors using the L_∞ and L_2 norms of the CCM with those of the BCM for $q = 1$ and $b = 2$ for Example 4 in Table 9. We clearly observe that achieving the desired level of accuracy is more effectively accomplished with the CCM compared to the BCM. Furthermore, Figure 4 illustrates a comparison of residual errors between the current technique and the BCM, revealing that the residual errors of the CCM are significantly lower than those of the BCM.

Table 9. Comparison of errors using the L_∞ and L_2 norm for $q = 1$ and $b = 2$ in Equation (46).

n	L_∞		L_2	
	CCM	BCM	CCM	BCM
3	1.87×10^{-4}	3.96×10^{-3}	3.55×10^{-4}	6.63×10^{-3}
4	6.95×10^{-6}	7.11×10^{-4}	1.22×10^{-5}	1.34×10^{-3}
5	2.51×10^{-7}	5.20×10^{-4}	3.82×10^{-7}	8.82×10^{-4}
6	6.62×10^{-9}	1.71×10^{-4}	1.09×10^{-8}	3.13×10^{-4}
7	1.85×10^{-10}	1.38×10^{-4}	2.98×10^{-10}	2.56×10^{-4}
8	5.25×10^{-12}	6.20×10^{-5}	7.68×10^{-12}	1.15×10^{-4}
9	9.90×10^{-14}	4.84×10^{-5}	1.71×10^{-13}	1.02×10^{-4}
10	1.42×10^{-15}	2.79×10^{-5}	2.97×10^{-15}	5.33×10^{-5}

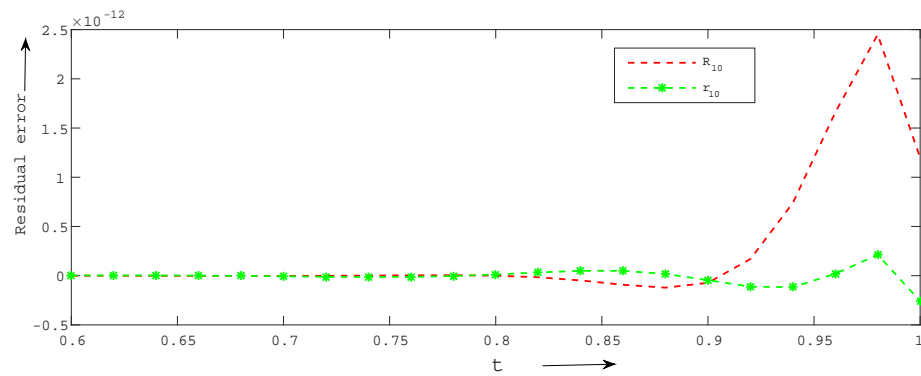


Figure 4. Comparison of residual errors obtained by the CCM and the BCM for Example 4.

Example 5. Consider a numerical problem without exact solution

$$\begin{cases} (t^2 w')' = t^2 \frac{0.76129 w}{w + 0.03119}, & t \in (0, 1), \\ w'(0) = 0, \quad 5w(1) + w'(1) = 5. \end{cases} \tag{47}$$

Its equivalent form is

$$w(t) = \frac{\beta_3}{\beta_1} + \int_0^1 \kappa(t, \zeta) \zeta^2 \left(\frac{0.76129 w(\zeta)}{w(\zeta) + 0.03119} \right) d\zeta, \quad t \in (0, 1),$$

where

$$\kappa(t, \zeta) = \begin{cases} (1 - \frac{1}{\zeta}) - \frac{1}{5}, & t \leq \zeta, \\ (1 - \frac{1}{t}) - \frac{1}{5}, & \zeta \leq t \end{cases}$$

and $b = 2, \beta_1 = 5, \beta_2 = 1, \beta_3 = 5$.

We compare the absolute difference of estimated solutions ($E_{45} = \|w_4 - w_5\|$) of the CCM with the BCM in Table 10. It can be seen from the table that fewer errors in numerical solutions are obtained by the present method than the BCM [39].

Table 10. Comparison of the numerical results of Equation (47).

t	CCM			BCM [39]		
	w ₄	w ₅	E ₄₅	w ₄	w ₅	E ₄₅
0.1	0.82970609	0.82970609	8.53 × 10 ⁻¹⁰	0.82970610	0.82970609	5.21 × 10 ⁻⁹
0.2	0.83337473	0.83337473	6.07 × 10 ⁻¹⁰	0.83337474	0.83337473	6.83 × 10 ⁻⁹
0.3	0.83948991	0.83948991	3.37 × 10 ⁻¹⁰	0.83948992	0.83948991	4.07 × 10 ⁻⁹
0.4	0.84805278	0.84805278	1.22 × 10 ⁻¹⁰	0.84805279	0.84805278	4.58 × 10 ⁻¹⁰
0.5	0.85906492	0.85906492	1.06 × 10 ⁻¹⁰	0.85906493	0.85906493	1.09 × 10 ⁻⁹
0.6	0.87252832	0.87252831	7.50 × 10 ⁻¹¹	0.87252832	0.87252832	4.46 × 10 ⁻¹⁰
0.7	0.88844530	0.88844530	6.95 × 10 ⁻¹¹	0.88844531	0.88844531	4.49 × 10 ⁻¹⁰
0.8	0.90681854	0.90681854	2.15 × 10 ⁻¹¹	0.90681855	0.90681855	2.70 × 10 ⁻¹⁰
0.9	0.92765098	0.92765098	1.82 × 10 ⁻¹¹	0.92765099	0.92765099	2.35 × 10 ⁻⁹
1.0	0.95094579	0.95094579	1.28 × 10 ⁻¹¹	0.95094580	0.95094580	2.90 × 10 ⁻⁹

7. Conclusions

We employed an efficient technique to approximate the numerical solution of Emden–Fowler-type SBVPs with derivative dependence. This approach utilizes the collocation technique based on Chebyshev polynomials, considering the equivalent Fredholm integral form. The major advantage of the current technique is its ability to reach the requisite level

of accuracy compared to previously established methods, such as the BCM [34]. Under quite general conditions, an error analysis was established to assess the accuracy of the current technique. To validate this accuracy, we considered various numerical examples to compute the maximum absolute errors using the L_∞ and L_2 norms. These results were then compared with those of the existing BCM method [34], demonstrating that the current approach is superior. Moreover, a graphical comparison of residual errors between the CCM and the BCM illustrates that the residual errors of the CCM are significantly lower than those of the BCM. Overall, the current method (CCM) renders a promising and accurate solution of these types of mathematical problems. The proposed techniques can be extended to solve systems of higher-order singular differential equations with a set of local and nonlocal boundary conditions. Additionally, the presented collocation techniques can be applied to gain insights into nonlinear singular pantograph delay differential models arising in various natural and physical phenomena. Furthermore, the current approach can be applied to solve Fredholm–Volterra-type integro-differential equations and fractional Lane–Emden–Fowler-type equations.

Author Contributions: Conceptualization, S.K. and A.K.S.; Methodology, S.K. and A.K.S.; Validation, S.K., A.K.S. and U.G.; Formal analysis, S.K., A.K.S. and U.G.; Writing—original draft, S.K. and A.K.S.; Writing—review and editing, S.K., A.K.S. and U.G.; Supervision, A.K.S. All authors contributed equally. All authors have read and agreed to the published version of the manuscript.

Funding: This research received no external funding.

Data Availability Statement: No new data were created or analyzed in this study. Data sharing is not applicable to this article.

Acknowledgments: The authors are thankful to the reviewers for their valuable suggestions to improve the manuscript.

Conflicts of Interest: The authors declare no conflicts of interest.

References

- Bobisud, L.; O'Regan, D. Positive solutions for a class of nonlinear boundary value problems at resonance. *J. Math. Anal. Appl.* **1994**, *184*, 263–284. [[CrossRef](#)]
- Van Gorder, R. Exact first integrals for a Lane-Emden equation of the second kind modeling a thermal explosion in a rectangular slab. *New Astron.* **2011**, *16*, 492–497. [[CrossRef](#)]
- Reger, K.; Van Gorder, R. Lane-Emden equations of second kind modelling thermal explosion in infinite cylinder and sphere. *Appl. Math. Mech.* **2013**, *34*, 1439–1452. [[CrossRef](#)]
- Gray, B. The distribution of heat sources in the human head—Theoretical considerations. *J. Theor. Biol.* **1980**, *82*, 473–476. [[CrossRef](#)] [[PubMed](#)]
- McElwain, D. A re-examination of oxygen diffusion in a spherical cell with Michaelis-Menten oxygen uptake kinetics. *J. Theor. Biol.* **1978**, *71*, 255–263. [[CrossRef](#)] [[PubMed](#)]
- Rachnková, I.; Koch, O.; Pulverer, G.; Weinmuller, E. On a singular boundary value problem arising in the theory of shallow membrane caps. *J. Math. Anal. Appl.* **2007**, *332*, 523–541. [[CrossRef](#)]
- Bartoshevich, M. A heat-conduction problem. *J. Eng. Phys.* **1975**, *28*, 240–244. [[CrossRef](#)]
- Galdi, G.P.; Pileckas, K.; Silvestre, A.L. On the unsteady Poiseuille flow in a pipe. *Z. Angew. Math. Phys.* **2007**, *58*, 994–1007. [[CrossRef](#)]
- Ding, H.; Wang, H.; Chen, W. Analytical solution for the electro elastic dynamics of a non homogeneous spherically isotropic piezoelectric hollow sphere. *Arch. Appl. Mech.* **2003**, *73*, 49–62. [[CrossRef](#)]
- Chandrasekhar, S. An introduction to the study of stellar structure. *Ciel Terre* **1939**, *55*, 412.
- Bobisud, L. Existence of solutions for nonlinear singular boundary value problems. *Appl. Anal.* **1990**, *35*, 43–57. [[CrossRef](#)]
- Dunninger, D.; Kurtz, J.C. Existence of solutions for some nonlinear singular boundary value problems. *J. Math. Anal. Appl.* **1986**, *115*, 396–405. [[CrossRef](#)]
- Yan, B.; O'Regan, D.; Agarwal, R. Positive solutions for second order singular boundary value problems with derivative dependence on infinite intervals. *Acta Appl. Math.* **2008**, *103*, 19–57. [[CrossRef](#)]
- Pandey, R.K.; Verma, A.K. Existence-uniqueness results for a class of singular boundary value problems-II. *J. Math. Anal. Appl.* **2008**, *338*, 1387–1396. [[CrossRef](#)]
- Pandey, R.K.; Verma, A.K. Existence-uniqueness results for a class of singular boundary value problems arising in physiology. *Nonlinear Anal. Real World Appl.* **2008**, *9*, 40–52. [[CrossRef](#)]

16. Pandey, R.K.; Verma, A.K. On solvability of derivative dependent doubly singular boundary value problems. *J. Appl. Math. Comput.* **2010**, *33*, 489–511. [[CrossRef](#)]
17. Kanth, A.R. Cubic spline polynomial for non-linear singular two-point boundary value problems. *Appl. Math. Comput.* **2007**, *189*, 2017–2022.
18. Chawla, M.M.; Katti, P.C. Finite difference methods and their convergence for a class of singular two point boundary value problems. *Numer. Math.* **1982**, *39*, 341–350. [[CrossRef](#)]
19. Russell, R.D.; Shampine, L.F. Numerical methods for singular boundary value problems. *SIAM J. Numer. Anal.* **1975**, *12*, 13–36. [[CrossRef](#)]
20. Iyengar, S.R.K.; Jain, P. Spline finite difference methods for singular two point boundary value problems. *Numer. Math.* **1986**, *50*, 363–376. [[CrossRef](#)]
21. Kumar, M. A three-point finite difference method for a class of singular two-point boundary value problems. *J. Comput. Appl. Math.* **2002**, *145*, 89–97. [[CrossRef](#)]
22. Verma, A.K.; Kayenat, S. On the convergence of Mickens' type nonstandard finite difference schemes on Lane-Emden type equations. *J. Math. Chem.* **2018**, *56*, 1667–1706. [[CrossRef](#)]
23. Singh, R.; Kumar, J.; Nelakanti, G. New approach for solving a class of doubly singular two-point boundary value problems using Adomian decomposition method. *Adv. Numer. Anal.* **2012**, *2012*, 541083. [[CrossRef](#)]
24. Singh, R.; Kumar, J.; Nelakanti, G. Numerical solution of singular boundary value problems using Green's function and improved decomposition method. *J. Appl. Math. Comput.* **2013**, *43*, 409–425. [[CrossRef](#)]
25. Singh, R.; Kumar, J. Solving a class of singular two-point boundary value problems using new modified decomposition method. *ISRN Comput. Math.* **2013**, *2013*, 262863. [[CrossRef](#)]
26. Singh, R.; Kumar, J.; Nelakanti, G. Approximate series solution of singular boundary value problems with derivative dependence using Green's function technique. *Comput. Appl. Math.* **2014**, *33*, 451–467. [[CrossRef](#)]
27. Singh, R.; Kumar, J. An efficient numerical technique for the solution of nonlinear singular boundary value problems. *Comput. Phys. Commun.* **2014**, *185*, 1282–1289. [[CrossRef](#)]
28. Singh, R.; Kumar, J. The Adomian decomposition method with Green's function for solving nonlinear singular boundary value problems. *J. Appl. Math. Comput.* **2014**, *44*, 397–416. [[CrossRef](#)]
29. Marinca, V.; Dehghan, M. Four techniques based on the B-spline expansion and the collocation approach for the numerical solution of the Lane-Emden equation. *Math. Methods Appl. Sci.* **2011**, *36*, 2243–2253.
30. Roul, P.; Goura, V.M. B-spline collocation methods and their convergence for a class of nonlinear derivative dependent singular boundary value problems. *Appl. Math. Comput.* **2019**, *341*, 428–450. [[CrossRef](#)]
31. Turkyimazoglu, M. Solution of initial and boundary value problems by an effective accurate method. *Int. J. Comput. Methods* **2017**, *14*, 1750069. [[CrossRef](#)]
32. Roul, P. Doubly singular boundary value problems with derivative dependent source function: A fast-converging iterative approach. *Math. Methods Appl. Sci.* **2019**, *42*, 354–374. [[CrossRef](#)]
33. Roul, P.; Goura, V.P.; Agrawal, R. A new high order numerical approach for a class of nonlinear derivative dependent singular boundary value problems. *Appl. Numer. Math.* **2019**, *145*, 315–341. [[CrossRef](#)]
34. Shahni, J.; Singh, R. Numerical results of Emden-Fowler boundary value problems with derivative dependence using the Bernstein collocation method. *Eng. Comput.* **2022**, *38*, S371–S380. [[CrossRef](#)]
35. Sastry, S.S. *Introductory Methods of Numerical Analysis*; PHI Learning Pvt. Ltd.: New Delhi, India, 2005.
36. Powell, M.J.D. *Approximation Theory and Methods*; Cambridge University Press: Cambridge, UK, 1981.
37. Voronovskaya, E. Dtermination de la forme Asymptotique Dapproximation des Fonctions par les polynmes de M. Bernstein *Doklady. Akad. Nauk. Sssr* **1932**, *79*, 79–85.
38. Lorentz, G.; DeVore, R. *Constructive Approximation, Polynomials and Splines Approximation*; Springer: Berlin, Germany, 1993.
39. Shahni, J.; Singh, R. An efficient numerical technique for Lane-Emden-Fowler boundary value problems: Bernstein collocation method. *Eur. Phys. J. Plus* **2020**, *135*, 475. [[CrossRef](#)]

Disclaimer/Publisher's Note: The statements, opinions and data contained in all publications are solely those of the individual author(s) and contributor(s) and not of MDPI and/or the editor(s). MDPI and/or the editor(s) disclaim responsibility for any injury to people or property resulting from any ideas, methods, instructions or products referred to in the content.